

# A Deep Neural Network for SSVEP-based Brain-Computer Interfaces

Osman Berke Guney, Muhtasham Oblokulov and Huseyin Ozkan, *Member, IEEE*

**Abstract**—Target identification in brain-computer interface (BCI) spellers refers to the electroencephalogram (EEG) classification for predicting the target character that the subject intends to spell. When the visual stimulus of each character is tagged with a distinct frequency, the EEG records steady-state visually evoked potentials (SSVEP) whose spectrum is dominated by the harmonics of the target frequency. In this setting, we address the target identification and propose a novel deep neural network (DNN) architecture. The proposed DNN processes the multi-channel SSVEP with convolutions across the sub-bands of harmonics, channels, time, and classifies at the fully connected layer. We test with two publicly available large scale (*the benchmark and BETA*) datasets consisting of in total 105 subjects with 40 characters. Our first stage training learns a global model by exploiting the statistical commonalities among all subjects, and the second stage fine tunes to each subject separately by exploiting the individualities. Our DNN strongly outperforms the state-of-the-art on both datasets, by achieving impressive information transfer rates *265.23 bits/min* and *196.59 bits/min*, respectively, with only 0.4 seconds of stimulation. To our best knowledge, our rates are the highest ever reported performance results on these datasets. The code is available for reproducibility at <https://github.com/osmanberke/Deep-SSVEP-BCI>.

**Index Terms**—Deep learning, Brain-computer interface, BCI, Steady state visually evoked potentials, SSVEP, Speller



## 1 INTRODUCTION

RAIN-computer interfaces (BCIs) [1], [2] set up a direct communication channel between the human brain and a computer to translate brain signals to external commands. BCIs have received increasing attention in recent years and led to substantial progress [3] in many applications such as stroke rehabilitation [4], gaming [5], robot and cursor control [6], [7]. Another prominent application is the BCI speller [1] that assists patients with severe motor disabilities (e.g. amyotrophic lateral sclerosis), so that they can communicate by spelling via solely brain signals without (or with limited) muscular activity. BCI speller research is recently more focused on the use of steady-state visually evoked potentials (SSVEP) in EEG (Electroencephalogram) signals [8], [9] as the SSVEP is of relatively higher signal-to-noise ratio (SNR) than, for instance, the event related potentials (ERP) in P300 spellers [10]. Consequently, BCI SSVEP spellers achieve higher information transfer rate (ITR) with ease of system configuration and relatively little time for training [11], [12].

The steady-state brain response to a visual stimulus flickering at a certain frequency induces the SSVEP signal that is characteristically dominated in its spectrum by the harmonics of the applied input flickering frequency. This enables the use of SSVEP in BCI speller designs [13]. In the experimental paradigm of BCI SSVEP spellers, a matrix of certain alphanumeric characters, each of which flickers at a unique frequency, is presented on the computer screen (Fig. 1) and the subject attends to the character that she/he intends to spell. The goal is to predict (i.e. identify) the in-

tended (i.e. targeted) character based on the received SSVEP signal while managing the trade-off between the prediction accuracy and the signal duration (i.e. spelling speed) such that the maximum ITR is achieved. Since the frequency spectrum is typically exploited up to almost 100 Hz with the largest harmonic, a high temporal precision and at least 200 Hz sampling rate are necessary. Hence, EEG is a popular and appropriate choice for its high speed acquisition with a non-invasive and low cost implementation [14], [15].

We address the target identification in BCI SSVEP speller systems as a multi-class classification problem, and propose a deep neural network (DNN) architecture to the goal of ITR maximization. The proposed DNN processes SSVEP signals in time domain as an end-to-end system from the EEG to the prediction of the targeted character. Our DNN architecture significantly outperforms the state-of-the-art as well as the most recently proposed techniques in the literature. We achieve *impressive ITRs with only 0.4 seconds of stimulation, 265.23 bits/min and 196.59 bits/min*, on the two publicly available large scale benchmark [16] and BETA [17] datasets that consist of the EEG data of 105 subjects with 40 target characters. *To our best knowledge, these are the highest ever ITRs reported on these datasets.* Moreover, the proposed DNN can be straightforwardly extended (as it is not specific to spellers) to general BCI systems for the broader purpose of translating brain signals to external commands. Therefore, we believe that our technique will produce a great impact and an immensely valuable use in plethora of real-life applications of SSVEP-based BCIs such as rehabilitation, control and gaming.

### 1.1 Related Work

One of the conventional target character identification methods in the literature is based on the power spectrum density

- Osman Berke Guney and Huseyin Ozkan are with the Faculty of Engineering and Natural Sciences at Sabanci University, Istanbul, Turkey. Email: {osmanberke, huseyin.ozkan}@sabanciuni.edu. Muhtasham Oblokulov is with the Technical University of Munich, Munich, Germany. Email: muhtasham.oblokulov@tum.de. This work was supported by The Scientific and Technological Research Council (TUBITAK) of Turkey under Contract 118E268.



combining the results afterwards is shown to significantly increase the identification performance of the Standard-CCA method. The reason for this improvement is that the filter-bank approach evaluates the contribution (to the identification) of each harmonic degree separately by using various sub-bands in the spectrum. This is supported in [32] by that, as the degree increases, the harmonic magnitude drops but the SNR does not necessarily decrease since the noise reduces faster. We refer to the figure 7 of [32] for a demonstration, where it is shown that the harmonics up to 50 Hz (up to the 3rd-5th harmonics in our case) maintains a relatively high SNR. We also observe this -by inspection- in our own signal analysis (cf. the spectrum example provided in Fig. 1 in the case of the harmonics of 10 Hz up to the 3rd degree). The filter-bank approach has become a standard procedure thereafter and many researchers have followed by utilizing it to increase the performance [8], [9], [12], [33].

The correlated component analysis (**CORRCA**) [9] maximizes the correlation between the multi-channel template signals (which are calculated by averaging the SSVEP signals across multiple trials in the training set for each frequency) and the multi-channel test signal, and then the frequency of the highest correlation yields the final prediction<sup>2</sup> [9]. The maximization in CORRCA [9] is with respect to a single projection across channels, whereas the maximization in Standard-CCA [20] is with respect to two projections one of which is across channels and the other is across harmonics in the references. As for the several extensions of CORRCA, the filter bank approach is used in FBCORRCA [9], the information from other correlation coefficients (besides the largest one) is exploited via carefully fusing them with exponentially decaying weights in HFCORRCA [34], and spatial filters of all stimulus frequencies are utilized in TSCORRCA [9] yielding the best performing extension. A method called task related component analysis (TRCA) is used for BCI SSVEP spellers in [8]. The formulation models the SSVEP signal as a task-related information signal that is linearly contaminated with noise. It is shown in [8] that **TRCA**, when used for suppressing the noise in SSVEP by maximizing the inter-trial covariance and thus extracting informative components, delivers higher ITR performance than the Extended-CCA method. TRCA for speller can be enhanced by the filter bank approach along with spatial filters yielding the Ensemble-TRCA (**eTRCA**) technique [8]. A multi stimulus scheme (**ms-eTRCA**) is further incorporated in [33] which is an advancement over the techniques Extended-CCA and eTRCA. There exists a few deep learning based BCI SSVEP speller studies [35], [36], [37], [38], [39], [40]. For example, a DNN is applied in [35], compared with CCA based methods, and observed to yield a better identification performance. Unlike [35], our proposed DNN receives the data directly in time (i.e. not in the frequency domain). In contrast to [35] that is trained only once based

<sup>2</sup>Since each character corresponds by design to a unique frequency, we use the phrases “target character” or “frequency” and “identification” or “prediction” or “classification” interchangeably depending on the context. Also, we refer to the person using a BCI speller as the “user”, and the person participating in an SSVEP EEG experiment as the “subject”. The word “experiment” is reserved for an EEG experiment, and we name our testing of algorithms as “performance evaluations”. For a frequency  $f$ , we refer to all integer multiples as the “harmonic”, including the fundamental frequency  $f$  itself as the first harmonic.

on all the data from all of the subjects without a dropout regularization; our DNN is empowered with dropout layers during training and is also optimized with respect to each subject separately to take into account the statistical differences across subjects. To be more specific, we train our DNN in two stages. We first train globally across all subjects in the first stage, and then fine tune it down to each subject by re-training the same DNN initialized with the globally trained previous model in the second stage. As a result, each subject in our work has its own model. More importantly, our DNN is tested with two far larger benchmark datasets. One of them includes 35 subjects [16] and the other includes 70 subjects [17], both with 40 targets. Whereas not only the DNN in [35] but also the recurrent neural networks of [39], [40] are only tested with at most 5 targets and 11 subjects despite that an effective speller requires as many targets as the size of the alphabet. Therefore, the networks of [35], [39], [40] are not applicable in the realistic scenarios of spellers; and are also not tested statistically robustly since their data is fairly limited. On the contrary, our DNN is directly applicable in realistic scenarios, and statistically robustly and repeatedly observed to provide impressive ITRs.

The deep learning approach in [36] demonstrates a lower identification performance on the benchmark dataset [16] when compared to the state-of-the-art (i.e. when compared to the correlation and component analyses and their several extensions for enhancement such as sub-band combinations, spatial filtering, noise suppression and individual data). The idea of the second stage in our DNN training (fine tuning with transfer learning) has also been used in [36] based on, though, only 2 subjects (other 33 subjects of the dataset [16] are skipped). A different training scheme is introduced in [37], where a DNN is trained with the data from a specific training set of subjects and then tested on another subject that is excluded in the training. This removes the burden of calibration, i.e., adaptation, to subject in the phase of deploying a speller system but at the same time it is certainly sub-optimal as the statistics change from one subject to another. Moreover, as a user uses a BCI SSVEP speller system, she/he accumulates over time her/his own data which should certainly be exploited. Hence, a better strategy is to transfer a pre-trained model and continuously improve it as new personal data becomes available. Indeed, subject specific adaptation has been observed in [38] to largely improve the identification performance. For this reason, in the presented study, we use adaptation by training first globally across all subjects and later transferring it to each subject separately, yielding the proposed two-stage learning. One further conclusion in [38] is that the state-of-the-art conventional techniques (defined by the conventional correlation and component analyses based approaches) perform better than the deep learning based approaches. We attribute this to that the deep learning has yet to be explored. In fact, we prove the opposite since our proposed DNN in this study significantly outperforms all of the state-of-the-art as well as the most recently proposed techniques.

## 1.2 Novel Contributions and Highlights

We propose a novel deep neural network architecture for a BCI SSVEP speller, which strongly outperforms (with uni-

formly the highest ITR results across all durations, i.e., signal lengths, of stimulation) the state-of-the-art as well as the most recently proposed competing techniques. Our performance evaluations are based on two publicly available large scale datasets that consist of 105 subjects in total with 40 target characters. In these performance evaluations, we focus on comparing with 9 existing prominent techniques that had previously reported relatively high ITRs. *The code, link to the datasets and the proposed DNN model are all available for reproducibility at <https://github.com/osmanberke/Deep-SSVEP-BCI>.*

- The proposed DNN architecture achieves, with only 0.4 seconds of stimulation, 265.23 bits/min and 196.59 bits/min ITRs on the benchmark [16] and BETA [17] datasets. Our ITRs are the highest ever reported performance results on these datasets to date.
- The presented study is the first to observe statistically robustly the efficacy of deep learning in BCI SSVEP spellers by improving the state-of-the-art significantly via the proposed DNN. Note that deep learning, despite its great success in many fields such as image recognition [41] and natural language processing [42], seems to have been limitedly explored in BCI SSVEP spellers. A few number of existing deep learning studies (e.g. [36], [38]) had not even succeeded to match the performance of the conventional approaches (e.g. [29], [31]).
- EEG signals are well-known to exhibit data statistics that can drastically change from one subject to another in various aspects (e.g. weights of the SSVEP harmonics) but also share similarities in certain other aspects (e.g. SSVEP being tuned to the frequency of stimulation) [43], [44]. To exploit the commonalities while tackling variations, the proposed DNN is trained with a two-staged approach. The first stage trains with all the available SSVEP data from all the subjects, and then the resulting DNN model of the first stage with a global view is transferred to the second stage that fine-tunes to each subject separately. This idea of transfer learning had been preliminarily used in [36] for BCI SSVEP spellers, where some initial results are provided for only 2 subjects. Here, we extend to all of the available 105 subjects, and observe its (fine tuning with transfer learning) benefit statistically more robustly with as large as two-fold ITR improvements.
- In most of the techniques in the BCI SSVEP speller literature, conventionally, 9 EEG channels (Pz, PO3, PO5, PO4, PO6, POz, O1, Oz, and O2) are placed over the occipital and parietal regions. Even though these channels provide perhaps the most informative SSVEP signals [45], other channels might certainly be informative as well. To this end, our proposed DNN is fed with all the available channels (64 in our case) and learns an optimal combination across channels (hence yielding an optimal set of channels after sorting with respect to the combination weights); and this is even for each subject separately taking into account that the optimal combination can change across subjects. In fact, we observe a statistically significant improvement (by about 20 bits/min on the benchmark dataset [16] and 10 bits/min on the BETA dataset [17]) in ITR compared to the conventional pre-determined set of 9 channels.

Therefore, a manual channel selection or running an independent algorithm for that is not required in our method. We also present the topographic channel distributions with respect to the combination weights.

- Unlike the competing techniques (e.g., [12], [31], [34]), neither the EEG channel selection nor the harmonics combination in our method is manual or rule based. Rather, we jointly learn the both (spatial filtering across channels and combining the sub-bands of harmonics) with the proposed DNN in a completely data driven manner. Optimizing the sub-band combination is important since the harmonics can have significantly different magnitudes and different contributions (not necessarily proportional to the magnitude) to the target identification. For instance, higher order harmonics having low magnitude does not necessarily mean that they have low contribution, since the SNR might be high despite the low magnitude (cf. [32] and also our Fig. 1). Hence, a normalization across frequency bands via a weighted sub-band combination is implemented in the first layer of our DNN. This improves the target identification accuracy by about 2% in the benchmark dataset [16] and 2.5% in the BETA dataset [17] (both at only 0.4 second of signal acquisition), where note that the chance level is  $1/40 = 2.5\%$ .

In the following Section 2 and Section 3, we provide the problem description and the proposed DNN as our solution. After we present the performance evaluations in Section 4, the paper concludes in Section 5 with final remarks.

## 2 PROBLEM DESCRIPTION

During a trial in a BCI SSVEP speller session (illustrated in Fig. 1), the subject is visually presented a matrix of  $M$  alphanumeric characters each of which flickers at unique frequency  $f_j : j \in \mathcal{M} = \{1, 2, \dots, M\}$  (in Hz). Then, she/he is asked to concentrate on the target character with the identification number  $y \in \mathcal{M}$  that is to be spelled. The brain response, as a result of the stimulation by the intended target character  $y$  flickering at the frequency  $f_y$ , is measured with EEG as the multi-channel SSVEP signal  $x \in \mathbb{R}^{C \times N}$ . Here,  $C$  is the number of channels and  $N = T \times f_s$  is the number of samples in each channel (with  $T$  and  $f_s$  being the signal or stimulation duration in seconds and the sampling frequency in Hz, respectively).

We emphasize that a BCI SSVEP speller system is typically designed for enabling a severely motor disabled individual to *communicate flawlessly at a fast rate which requires a high speed accurate speller*. Therefore, the main design goal is to maximize the information transfer rate (ITR) [46] that is a function of the target identification accuracy and the stimulation duration. The target identification here refers to the prediction of the target character  $y$  based on the signal  $x$ . If this prediction is perfectly accurate, i.e., if the prediction accuracy is  $P = 1$ , then the trial-by-trial spelling of a length- $l$  word requires  $T \times l$  seconds which is equivalent to the ITR  $\log_2 M \frac{60}{T}$  bits per minute, i.e.,

$$\begin{aligned} \mathcal{I}(P, T) &= (\log_2 M + P \log_2 P + (1 - P) \log_2 \left[ \frac{1 - P}{M - 1} \right]) \frac{60}{T} \\ &= (\log_2 M) \frac{60}{T} \text{ (when } P = 1 \text{)}. \end{aligned}$$

Note that the prediction accuracy  $0 \leq P \leq 1$  is almost never perfect; nevertheless, if the identification method is optimal (with the minimum possible error rate, i.e.,  $1 - P$ ), then the accuracy  $P$  can be improved only by requesting a longer stimulation via increasing  $T$  (resulting in a longer SSVEP signal and hence a larger amount of data). However, in this case of lengthening the stimulation duration, the trials of the spelling slow down and consequently the information transfer rate (ITR) does not necessarily improve. For example, the long stimulation  $T = \infty$  (without habituating the subject) results in perfect accuracy  $P = 1$  that is, though, 0 ITR. Hence, when the identification method is optimal, it is not possible to expedite the spelling (shortening the stimulation duration  $T$  to spell in short time) while also improving the prediction accuracy  $P$  since the two are incompatible. This requires to manage a trade-off between  $P$  and  $T$  for the ITR maximization (in the ideal scenario of the optimal target identification). On the other hand, when the target identification is itself not optimal, improving the accuracy  $P$  is possible without increasing the stimulation duration  $T$  up to the point where the trade-off starts dominating.

In this paper, we not only manage the trade-off between the prediction accuracy  $P$  and the signal duration  $T$  but also obtain the optimal target identification for ITR maximization. Accordingly, we formulate the target character identification as a multi-class classification problem based on the data  $\{(x_i, y_i)\}_{i=1}^D$ , where  $D$  is the number of trials, to the goal of designing a classifier  $g(x) = \hat{y}$  for the above described prediction such that the ITR is maximized. Since the ITR maximization for a fixed  $T$  is equivalent to accuracy maximization, our strategy is to minimize the error rate  $1 - P$  for each  $T$  across a range of  $T$ 's, e.g.,  $T \in \{0.2, 0.3, \dots, 0.9, 1.0\}$  (optimizing the target identification separately for each  $T$ ), and observe the pair  $(P^*, T^*)$  that yields the maximum  $\mathcal{I}(P^*, T^*)$  (ITR maximization).

### 3 PROPOSED SOLUTION: A DNN ARCHITECTURE

In the following, we first briefly explain the SSVEP signal characteristics, and then describe the proposed deep neural network (DNN) architecture while also motivating its main design components.

#### 3.1 The SSVEP Signal

The stimulus in BCI SSVEP spellers characteristically leads to the SSVEP signal  $x$  (received through the EEG) that mostly comprises of the frequency components  $A_f \cos(2\pi ft + \phi_f)$  (where  $t = n/f_s$  due to sampling) at the harmonics<sup>2</sup>  $f = kf_y$  (integer  $k$ ) of the stimulation frequency  $f_y$ . The entire spectrum (up to typically 100 Hz as far as the information content, which is corrupted by the noise and interfered with other ongoing processes in the brain, is concerned) is surely spanned, but the components of the harmonics are larger, i.e.,  $A_{kf_y} \gg A_f > 0$  for  $f \neq kf_y$  [12], [13] (cf. also the spectrum example in Fig. 1). Then the target identification problem in this setting can be perhaps solved by the detection of the peaks across harmonics up to a certain degree in the Fourier spectrum of the received SSVEP signal. Namely, one can decide for the character whose harmonics are most covered by the received spectrum.

However, we emphasize that the harmonics are generally not observable in the spectrum as orthogonal components since the signal duration  $T$  yields only a low frequency resolution  $\delta\hat{\omega} = \frac{2\pi}{Tf_s}$  rad in normalized radian frequency and  $\delta f = \frac{\delta\hat{\omega}}{2\pi} f_s = \frac{1}{T}$  Hz in cyclic frequency (where  $T$  is short, e.g.,  $T = 0.4$  seconds). Therefore, the information in the harmonics of  $A_{k\delta f} \cos(2\pi k\delta f t + \phi_{k\delta f})$  (where  $t = n/f_s$  due to sampling) do leak onto the entire Fourier spectrum of the received SSVEP signal due to the correlation between the harmonics and the spectrum components. Thus, several variants of the canonical correlation analysis (CCA) can be used to find the flickering frequency (that the subject has been exposed to)  $f_{\hat{y}} : \hat{y} \in \mathcal{M}$  (and decide for the character  $\hat{y}$ ) which yields the maximum available correlation between the optimal (yielding that maximum) linear combination across channels in the received SSVEP signal and, for instance, A) the optimal linear combination of the corresponding reference harmonics, e.g., [12], [20], or B) the optimal linear combination across channels in the template SSVEP signals in the training set, e.g., [9], [34] and [8]. This is currently the essential principle in the state-of-the-art target identification techniques. We refer to Section 1.1 (Related Work) for a detailed discussion.

Despite being certainly impressive, we emphasize that, nevertheless, such state-of-the-art techniques do still have issues in various aspects. This presents an important opportunity for an improvement (once those issues are properly addressed) in terms of the state-of-the-art ITR performance. For example, the application of the CCA in its current form of those techniques does essentially measure the similarity between a test signal and each class mean of the respective training signals for obtaining a decision. This is sub-optimal as measuring the similarities to each training signal (rather than only mean) and then basing the decision on all such measured similarities would be a better approach (this resembles the difference between the nearest neighbor classifier and the nearest mean classifier). Also, CCA returns only a linear model whereas we observe in our performance evaluations that a nonlinear model is in fact needed.

To this end, in the following, we describe the proposed DNN while explaining how especially certain issues (the one mentioned above is only an example among many others) we have identified in the literature are resolved.

#### 3.2 The Proposed DNN Architecture

Our deep neural network (DNN) architecture operates as an end-to-end system which receives the multi-channel SSVEP signal  $x$  and processes it in a feed-forward manner to the final prediction of the target character as  $\hat{y}$ . The proposed DNN (Fig. 1) consists of 4 convolutional layers and 1 fully connected layer. Hence, we have the processing

$$x \rightarrow \text{Preprocessing: } [x^{(1)}, \dots, x^{(r)}, \dots, x^{(N_s)}] \rightarrow z_1 \\ \rightarrow z_2 \rightarrow z_3 \rightarrow z_4 \rightarrow s \rightarrow \hat{y} = \arg \max s(j),$$

where the preprocessing is for generating the sub-bands of harmonics  $[x^{(1)}, \dots, x^{(r)}, \dots, x^{(N_s)}]$  that are combined in the first layer to produce the output  $z_1$  which is subsequently processed in the second layer for spatial filtering across channels to produce the output  $z_2$ . Down-sampling follows in the third layer, yielding  $z_3$ , and then features are

extracted in the fourth layer as  $z_4$  passing to the classification in the fully connected layer to produce the prediction  $\hat{y} = \arg \max s(j)$  ( $s \in [0, 1]^{M \times 1}$  is the softmax output).

**Remark:** We point out that since there is only one nonlinear activation (ReLU) in the proposed DNN, it can be reduced to a single hidden layer feed-forward network again with the ReLU activation at the hidden layer. However, that would only lead to a non-intuitive complicated network. Here, in our proposed DNN, the information flow is natural through an intuitive and conceptually simple design. Therefore, we present the introduced network as the cascaded composition of 5 functionalities, i.e., layers (including the FC), for interpretability.

In the following, we describe our proposed DNN layer-by-layer. For each layer, we first motivate its use and then provide its definition. Afterwards, the training scheme and the further details are explained.

### 3.2.1 First layer for harmonics (sub-bands) combination

Under the stimulation by the target character flickering at the frequency  $f_y$ , the contributions of the harmonics to the generation of the SSVEP signal might vary from one harmonic to another. For example, a lower order harmonic generally has a larger magnitude compared to a higher degree one [12]. Nevertheless, since the higher order harmonics tend to be less (for example, compared to the alpha band around 10 Hz) interfered with other ongoing brain activities, they tend to manifest perhaps surprisingly a relatively high signal-to-noise ratio (SNR) [32] (as we also observe by inspection in the spectrum example of Fig. 1 in the case of the stimulation frequency 10 Hz up to the 3rd degree). We also refer to the study [32] for a general SNR investigation of SSVEP harmonics. However, it is not straightforward to assess which harmonic is more informative in the SSVEP classification, and hence how to normalize in the spectrum across the harmonics could be a fairly difficult task (although such a normalization is certainly required). This issue is handled in the literature by processing several sub-bands (such that each sub-band is designed to include only a certain set of harmonics) of the SSVEP spectrum separately, but then the results are fused in a rule based manner or are fused based on a fairly restrictive model, e.g., [12], [31], [34]. Therefore, how to choose the weight of a certain harmonic is not sufficiently addressed in the literature due to their manual handling.

In our DNN design, we opt to stay agnostic about this normalization of harmonics and instead let the network decide about the normalization weights by training in a completely data driven manner. For this purpose, we band-pass filter (denoted by  $\mathcal{G}_r$ , where we use MATLAB `filtfilt`<sup>3</sup> function) the SSVEP signal  $x \in \mathbb{R}^{C \times N}$  in each channel (multiple times  $1 \leq r \leq N_s$ ), where the lower cut-off is  $r \times \min\{f_j\} - \epsilon$  Hz (e.g.,  $\sim 8$  Hz for  $r = 1$  in both of the datasets [16], [17]) and the upper cut-off is  $6 \times \max\{f_j\} + \epsilon$  Hz (e.g.,  $\sim 90$  Hz in both of the datasets [16], [17]) with  $\epsilon$  being a small margin. The filter is designed as (using MATLAB `designfilt`<sup>3</sup> function) zero-phase Chebyshev-Type

1 with filter order 2 and 1 dB pass band ripple. Hence, each filter  $\mathcal{G}_r$  excludes the harmonics of the degree that is less than  $r$  while including the rest up to the 6'th degree (the maximum degree is set to 6 since beyond 100 Hz in the EEG is typically noise in BCIs). This yields the filtered output  $x^{(r)} \in \mathbb{R}^{C \times N}$  that includes a specific sub-band of harmonics.

The first layer of our proposed DNN (parameterized over the weights  $w_1 \in \mathbb{R}^{N_s \times 1}$ ) then produces a linear combination of these sub-bands for a normalization across the harmonics as  $z_1 = [x^{(1)}, \dots, x^{(r)}, \dots, x^{(N_s)}]w_1$ , where the input to the layer is  $[x^{(1)}, \dots, x^{(r)}, \dots, x^{(N_s)}] \in \mathbb{R}^{C \times N \times N_s}$  (i.e. a volume of  $9 \times 50 \times 3$  in the case of  $C = 9$ ,  $N = 50 = T \times f_s$  with  $T = 0.2$  seconds,  $f_s = 250$  Hz, and  $N_s = 3$ ) whereas the output is  $z_1 \in \mathbb{R}^{C \times N}$  (i.e., a plane of  $9 \times 50 \times 1$  when  $C = 9$  and  $N = 50$ ). Hence, our DNN has the capability to amplify the higher order harmonics (only if desired of course) by choosing the corresponding weights relatively high. In this first layer, the sub-band combination weights  $w_1$  are optimized.

### 3.2.2 Second layer for channel combination

The SSVEP signal is a multi-channel signal. The channels, on the one hand, bear valuable distinct information from the brain regions that they sense from but, on the other, produce signals that are also largely correlated. A combination across channels shall be considered to extract and accumulate the whole information while discarding the redundancy or non-informative variations (i.e. noise suppression). Also, multiple combinations are probably needed since extracting the information living in one subspace (of the complete channel space) can suppress the one living in another subspace. The required combinations might be even more than the number of channels as those informative subspaces are not necessarily orthogonal, requiring in return a nonlinear processing of combinations.

The existing CCA analyses in the literature (such as [8], [9], [12], [34]) allows a separate channel combination for each and every single test instance. We here criticise this since it not only A) creates an unnecessarily large degree of freedom and in return a large detrimental effect due to the induced strong proneness to overfitting, but also B) risks suppressing, in each case of the test instances, valuable information that can be extracted by other but not utilized combinations. To alleviate the issue B here, those techniques incorporate multiple combinations -for each and every testing again- by fusing the correlation coefficients of the CCA analysis, but this further worsens the issue A. Even then, the number of combinations is limited by the number of channels due to linearity, and the coefficient fusing is typically rule-based without a data-driven learning or is based on a simple fitting to a rather restrictive model. Further, a regularization step is generally not incorporated though it is certainly needed.

We, in the following, explain from another perspective to motivate our approach. Since the neural circuitry and nonlinear processes that are involved in brain to generate the SSVEP responses vary from lower degree harmonics (as well as intermodulations) to upper degree ones [47] (comparing, for instance, 12 Hz of the first degree with 60

<sup>3</sup><https://www.mathworks.com>

8.0Hz 0	9.0Hz 0.5π	10.0Hz π	11.0Hz 1.5π	12.0Hz 0	13.0Hz 0.5π	14.0Hz π	15.0Hz 1.5π
8.2Hz 0.5π	9.2Hz π	10.2Hz 1.5π	11.2Hz 0	12.2Hz 0.5π	13.2Hz π	14.2Hz 1.5π	15.2Hz 0
8.4Hz π	9.4Hz 1.5π	10.4Hz 0	11.4Hz 0.5π	12.4Hz π	13.4Hz 1.5π	14.4Hz 0	15.4Hz 0.5π
8.6Hz 1.5π	9.6Hz 0	10.6Hz 0.5π	11.6Hz π	12.6Hz 1.5π	13.6Hz 0	14.6Hz 0.5π	15.6Hz π
8.8Hz 0	9.8Hz 0.5π	10.8Hz π	11.8Hz 1.5π	12.8Hz 0	13.8Hz 0.5π	14.8Hz π	15.8Hz 1.5π

Fig. 2: The computer screen for the stimulus presentation in the experiments of the benchmark dataset is shown above (image is taken from [16]). This dataset consists of 64-channel SSVEP signals of 35 subjects. The stimulation frequency ranges in  $\{8, 8.2, \dots, 15.8\}$ , and phase difference between two adjacent frequencies is  $0.5\pi$ . The EEG experiment for each subject includes 6 blocks of 40 random-order trials (one trial per each character). The stimulation duration in each trial is 5 seconds (but we only use 1 second in our performance evaluations as 1 second is more than sufficient in our case) with an extra 0.5 seconds at the beginning for a visual cue and another 0.5 seconds at the end for an offset.

14Hz π	14.2Hz 1.5π	14.4Hz 0	14.6Hz 0.5π	14.8Hz π	15Hz 1.5π	15.2Hz 0	15.4Hz 0.5π	15.6Hz π	15.8Hz 0.5π	8.4Hz π
11.8Hz 1.5π	13Hz 0.5π	9.4Hz 1.5π	12Hz 0	12.4Hz π	13.4Hz 1.5π	12.6Hz 1.5π	10.2Hz 1.5π	11.4Hz 0.5π	11.6Hz π	
8.6Hz 1.5π	12.2Hz 0.5π	9.2Hz π	9.6Hz 0	9.8Hz 0.5π	10Hz π	10.4Hz 0	10.6Hz 0.5π	10.8Hz π		
13.6Hz 0	13.2Hz π	9Hz 0.5π	12.8Hz 0	8.8Hz 0	11.2Hz 0	11Hz 1.5π	8Hz 0			
			15.8Hz 1.5π				8.2Hz 0.5π			

Fig. 3: The computer screen for the stimulus presentation in the experiments of the BETA dataset is shown above (image is taken from [17]). This dataset consists of 64-channel SSVEP signals of 70 subjects. The stimulation frequency ranges in  $\{8, 8.2, \dots, 15.8\}$ , and phase difference between two adjacent frequencies is  $0.5\pi$ . The EEG experiment for each subject includes 4 blocks of 40 random-order trials (one trial per each character). The stimulation duration in each trial is 2 seconds (but we only use 1 second in our performance evaluations as 1 second is more than sufficient in our case) for the first 15 subjects (3 seconds for the remaining subjects) with an extra 0.5 seconds at the beginning for a visual cue and another 0.5 seconds at the end for an offset. Importantly, the target identification is more challenging in this case since the experiments are conducted outside of the laboratory environment thereby bearing lower SNR compared to the benchmark dataset.

Hz of the fifth degree), we certainly expect that different brain regions are more responsive to different harmonic degrees which necessitates the use of multiple spatial filters, i.e., channel combinations. Moreover, a different combination might be more appropriate to emphasize a certain stimulation frequency and its harmonics while suppressing the others which further necessitates multiple combinations for each class of observations.

Unlike the state-of-the-art existing methods, in our DNN

design, we use the same set of multiple channel combinations that is common for all of the training or test instances. This set in our study includes as many combinations as the number  $N_s$  of sub-bands for each stimulation frequency  $f_j$ , yielding in total, for instance,  $N_{ch} = 120 = N_s \times M$  combinations when  $N_s = 3$  and the number of characters is  $M = 40$ . We emphasize that if the number  $N_{ch}$  of channel combinations is more than the number  $C$  of channels, then one needs nonlinear processing (to avoid degeneracy and) to make use of the combinations effectively. Overall, this setting keeps the parameter complexity at a manageable level and mitigate the overfitting when compared to using a separate combination for each and every single test instance as in the existing techniques of literature. At the same time, our setting is also sufficiently powerful since we can use combinations as many as needed. To this end, the second layer (parameterized over the weights  $w_2 \in \mathbb{R}^{C \times N_{ch}}$ ) of our DNN implements the channel combinations by receiving the input plane  $z_1 \in \mathbb{R}^{C \times N}$  and returning the plane  $z_2 \in \mathbb{R}^{N \times N_{ch}}$ , i.e.,  $z_2 = z_1' w_2$ , where  $z_1'$  is the transpose of  $z_1$ . In order to achieve nonlinearity, we also apply the ReLU (rectified linear unit) activation but postpone it until the end of the third layer that follows the second layer for down-sampling with linear processing. In this second layer, the channel combination weights  $w_2$  are optimized.

### 3.2.3 Third layer for down-sampling and nonlinearity

The third layer has two functions. First, it reduces the parameter complexity in the network by down-sampling, i.e., stride 2, and also utilizes a simple two-tap filtering in time (with also a full third dimension along the depth) which is placed to represent the anti-aliasing filtering that is commonly used with down-sampling. The two-tap filtering in this layer additionally serves for roughly adjusting the spectral bandwidth for each information flow over the channel combinations in the network. Hence, multiple such two-tap filters (i.e.  $N_{ch} = 120$  many) are used. Second function of this layer is applying the nonlinearity. Note that when we have  $N_{ch} \gg C$ , the input plane of this third layer  $z_2 \in \mathbb{R}^{N \times N_{ch}}$  is rank-deficient with a rank at most  $C$  even if  $z_1 \in \mathbb{R}^{C \times N}$  (producing  $z_2 = z_1' w_2$ ) is full rank. This defeats the purpose of producing multiple channels combinations in the previous layer. Hence, in order to tackle the rank-deficiency and enable the effective use of the channel combinations, the third layer applies the nonlinear ReLU activation at the end after down-sampling to produce the output plane  $z_3 \in \mathbb{R}^{(N/2) \times N_{ch}}$ . In this third layer, the  $N_{ch}$  many two-tap filters are optimized.

### 3.2.4 Convolutional fourth and fully connected fifth layers

The fourth convolutional layer filters the input  $z_3$  with multiple finite impulse response filters (FIRs, each being of length 10 with also a full third dimension along the depth) to produce the features in  $z_4$  that is finally classified by the following fully connected (FC) layer. Hence, the very first input  $x$  is predicted as  $\hat{y} = \arg \max s(j)$  (note that  $s \in [0, 1]^{M \times 1}$  is the softmax output of the FC layer). The FIR filters in the fourth layer are expected to achieve frequency responses that are tuned to the spectral patterns of each stimulation class (1 FIR for each sub-band per each  $M = 40$  classes, yielding in total 120 filters when we have  $N_s = 3$

sub-bands) for extracting powerful features. Hence, in these two layers, all of the FIR filters (each being of length 10) as well as all of the FC weights are optimized. Note that all the layers in our DNN can be considered as convolutional: across sub-bands in the first, in space in the second (spatial filtering), in time in the third and fourth layers and across features in the last FC layer.

### 3.2.5 Two-staged training and further details

The proposed DNN is initialized by sampling the network weights (i.e. network parameters) from the Gaussian distribution with 0 mean and 0.01 variance, except that all of the weights in the first layer are initialized with 1's. We train the network in each iteration based on the training batch data  $\{(x_i, y_i)\}_{i=1}^{D_b}$ , where  $D_b$  is the number of trials in the batch, by minimizing the categorical cross entropy loss

$$\frac{1}{D_b} \sum_{i=1}^{D_b} -\log(s_i(y_i)) + \lambda \|\mathbf{w}\|^2$$

via the Adam optimizer [48] with the learning rate  $\nu = 0.0001$  (with no decaying), where  $\lambda$  is the constant of the L2 regularization which we set as  $\lambda = 0.001$ ,  $s_i \in [0, 1]^{M \times 1}$  is the softmax output of the FC layer for the instance  $x_i$ ,  $s_i(y_i)$  is the  $y_i$ 'th entry of  $s_i$  and the final prediction is  $\hat{y}_i = \arg \max s_i(j)$ . Here,  $\mathbf{w}$  represents all of the DNN weights (i.e. parameters). We also incorporate drop-outs between the second and third, third and fourth, and fourth and fifth layers with probabilities 0.1, 0.1, and 0.95, respectively.

We train the network in two stages. The first stage takes a global perspective by training with all of the data (ones in the training set) whereas the second stage re-initializes the network with the global model and fine-tunes it to each subject separately by training with only the corresponding subject data (of the training set). Hence, each subject has her/his own model. We note that, except a few, most of the existing studies do either develop only a local model or only a global model, which indicates that our introduced two-stage training is also a novel contribution to BCI SSVEP spellers (cf. Section 1.1 and Section 1.2 for detailed comparisons to the related work in the literature). We observe that this idea of transfer learning with two-staged learning, since it takes into account the inter-subject statistical variations, provides significant ITR improvements.

## 4 PERFORMANCE EVALUATIONS

We test our DNN on publicly available two large scale datasets which are the benchmark [16] and the BETA [17] datasets. The state-of-the-art techniques have been previously extensively tested on these datasets; and in our evaluations, we have compared against specifically those that have been reported to perform well. In particular, we have compared against 9 methods: Standard-CCA, ITCCA, Extended-CCA, m-Extended-CCA, CORRCA, TSCORRCA, TRCA, eTRCA and ms-eTRCA. In our comparisons, for fairness, we have strictly followed the same test procedures that have been used in these compared methods. Also, the performance results of the compared methods are directly transferred to here from their respective articles.

A BCI SSVEP speller experiment with a subject consists of several blocks, i.e., sessions, so that the subject can have a

break between two blocks and meanwhile the administrator can check the experiment setup. For example, there are 6 blocks and 4 blocks in the benchmark and BETA datasets, respectively, with 40 targets. In our performance evaluations, we conduct the comparisons (following the same exact procedure in the literature) in a leave-one-block-out fashion. For example, we train on 5 (or 3) blocks and test on the remaining block and repeat this process 6 (4) times in order to have exhaustively tested on each block in the case of the benchmark (or the BETA) dataset. Then, for each signal duration  $T$  in the range  $T \in \{0.2, 0.3, \dots, 0.9, 1.0\}$ , we report the mean multi-class classification accuracy as well as the mean ITR (information transfer rate) along with the standard errors. For fairness, we take into account a 0.5 seconds gaze shift time while computing the ITR results (in order to match to the way it is previously computed in other methods). We test with the pre-determined set of 9 channels (Pz, PO3, PO5, PO4, PO6, POz, O1, Oz, and O2) again for fair comparisons (since these are the channels that have been used in the compared methods), but we also test with all of the available 64 channels to fully demonstrate the efficacy of our DNN. In fact, we observe significant improvements with 64 channels over the pre-determined set. Confusion matrices for the stimulation frequencies (i.e. 40 classes of characters) are also presented for further insights into our multi-class classification accuracy results. Additionally, we have analyzed the effect of the number of sub-bands and the number of channels regarding the accuracy and ITR performance. We also report the topographic channel distributions to demonstrate the weight of each channel's contribution to the performance of our DNN.

In the following, we provide the details about the datasets and then present our results and discussions. We conclude afterwards.

**The benchmark dataset** has been recorded in BCI SSVEP speller experiments with 35 healthy subjects. Each experiment consists of 6 blocks, i.e., sessions. During a block, the subject is shown on the screen (Fig. 2) a matrix ( $5 \times 8$ ) of 40 target characters flickering at various frequencies (in the range 8 – 15.8 Hz with 0.2 Hz increments) with at least  $0.5\pi$  phase difference between adjacent frequencies. The EEG data is recorded through 64 channels. Each block includes 40 random-order trials (one trial per each target character). Each trial starts with a red square as a visual cue that is displayed for 0.5 seconds on the screen to guide subject's gaze to the desired target and then conducts the stimulation for 5 seconds that is followed by an offset of 0.5 seconds. Hence, each trial lasts 6 seconds. Subjects are instructed to avoid eye blinks to the best of their extent. The EEG is downsampled to 250 Hz and a notch filter at 50 Hz removes the common power-line noise. Average visual latency of the subjects is approximately estimated as 140 milliseconds in this dataset that essentially introduces a delay into the SSVEP signals. We refer to [16] for further details.

**The BETA dataset** and the benchmark dataset are similar, but do also have certain important differences. We note the differences of this BETA dataset in the following (the remaining attributes are exactly the same). This BETA dataset has been recorded in BCI SSVEP speller experiments with 70 healthy subjects. Each experiment consists of 4 blocks, i.e., sessions. The flickering target characters are shown in the

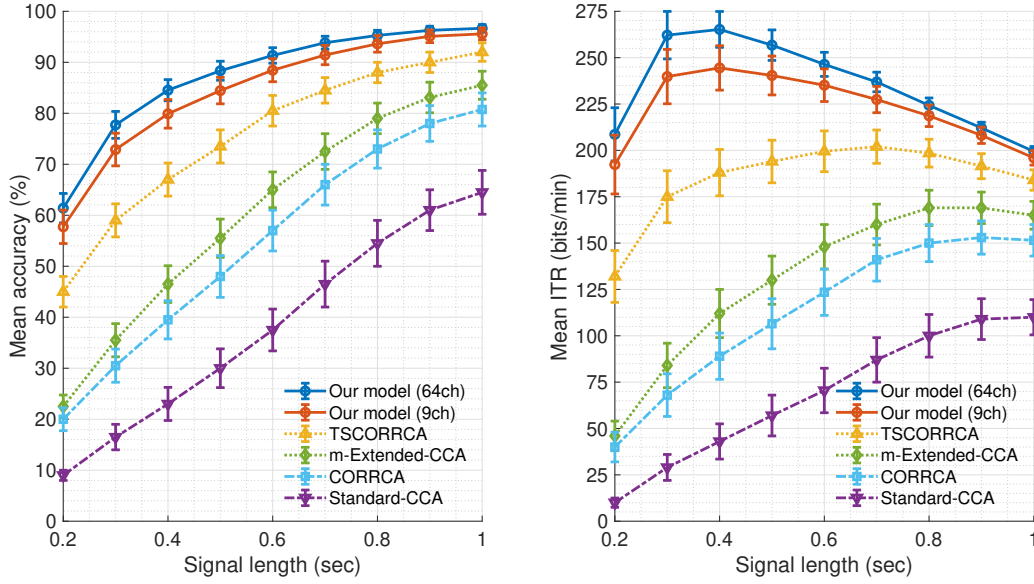


Fig. 4: The mean classification accuracy on the left and the mean information transfer rate (ITR) on the right are presented across all 35 subjects in this benchmark dataset, together with the standard errors indicated by the bars. The proposed DNN strongly outperforms all the competing algorithms uniformly for all stimulation durations, i.e., signal length  $T$ , while achieving the highest ITR of  $265.23 \text{ bits/min}$  with only a brief stimulation as short as 0.4 seconds when using 64 channels.

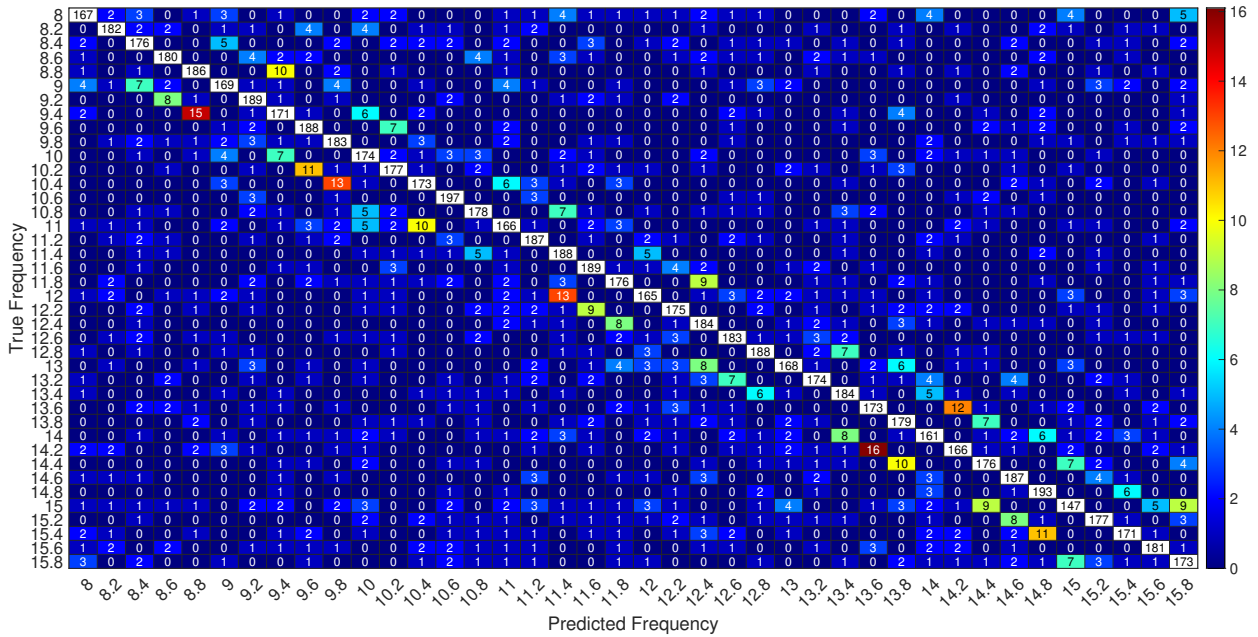


Fig. 5: The confusion matrix of the proposed DNN with the benchmark dataset with 64 channels at 0.4 seconds of stimulation.

form of a keyboard (Fig. 3). Importantly, the experiments are conducted outside of the laboratory environment, resulting in a lower SNR compared to the benchmark dataset. Hence, the target identification is more challenging in this case. The stimulation lasts 2 seconds for the first 15 subjects and 3 seconds for the remaining 55 subjects. Average visual latency of the subjects is approximately estimated as 130 ms in this dataset. We refer to [17] for further details.

Note that in this paper, we do not use the full duration of the SSVEP signals because using 0.4 seconds is already sufficient to achieve the maximum ITR which we extend though to 1 second to observe the overall behaviour.

Since the available data shrinks in the second stage

(shrinks more in the BETA dataset) of our DNN training, in order to achieve a better regularization, the probabilities of the first two drop-out layers are increased to 0.6 for the benchmark dataset [16] and to 0.7 for the BETA dataset [17]. The number of epochs are 1000 and 800 in the first stage for the benchmark dataset and the BETA dataset, respectively, where the batch size is 100 for the both. In the second stage, the number of epochs are the same and 1000 for both of the datasets and the batch sizes are 200 and 120 for the benchmark dataset and the BETA dataset, respectively. All the other settings of the proposed DNN are exactly the same (as defined previously) between the two stages and also between the two datasets. Hence, we

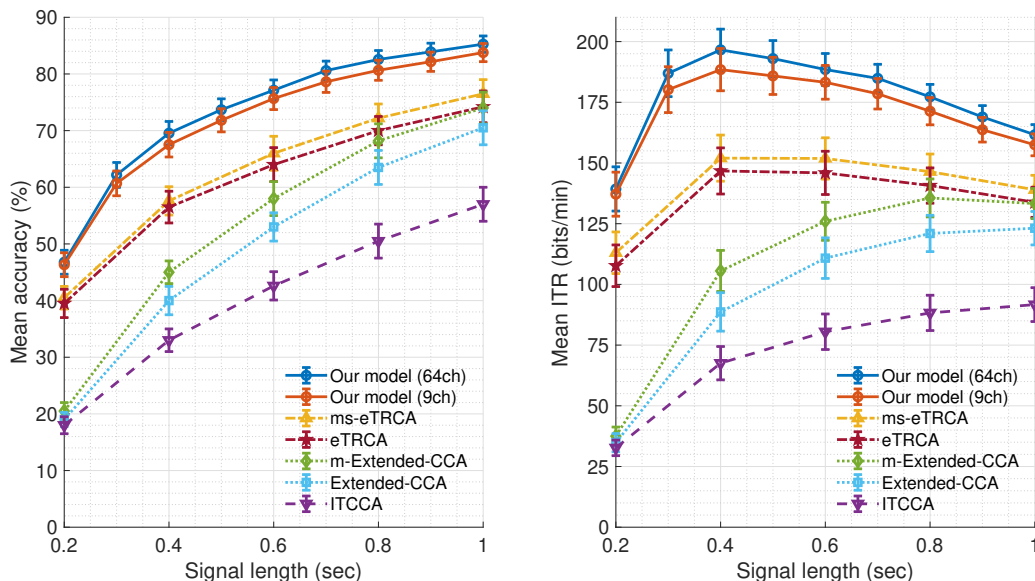


Fig. 6: The mean classification accuracy on the left and the mean information transfer rate (ITR) on the right are presented across all 70 subjects in this BETA dataset, together with the standard errors indicated by the bars. The proposed DNN strongly outperforms all the competing algorithms uniformly for all stimulation durations, i.e., signal length  $T$ , while achieving the highest ITR of 196.59 *bits/min* with only a brief stimulation as short as 0.4 seconds when using 64 channels.

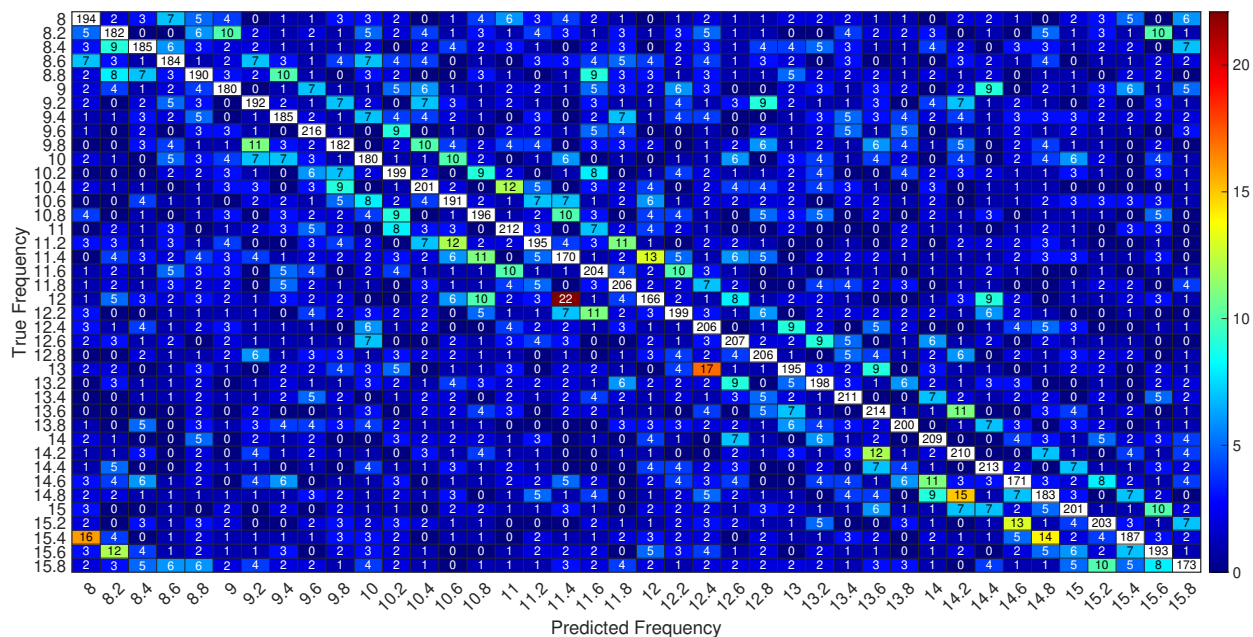


Fig. 7: The confusion matrix of the proposed DNN with the BETA dataset with 64 channels at 0.4 seconds of stimulation.

here particularly avoid fine tuning of the parameters to not overfit. The only exception perhaps appears when we specifically control a parameter such as the channel or sub-band number to analyze the corresponding effect on the ITR/accuracy performance.

#### 4.1 Results and Discussion

The proposed DNN is observed to achieve 265.23 bits/min ( $\sim 84\%$  accuracy with 64 channels) and 244.45 bits/min ( $\sim 80\%$  accuracy with 9 channels) maximum ITRs (cf. Fig. 4, alongside the corresponding confusion matrix in Fig. 5 with 64 channels and 0.4 seconds of stimulation) on the

benchmark dataset, and 196.59 ( $\sim 70\%$  accuracy with 64 channels) bits/min and 188.45 ( $\sim 68\%$  accuracy with 9 channels) bits/min on the BETA dataset (cf. Fig. 6, alongside the corresponding confusion matrix in Fig. 7 with 64 channels and 0.4 seconds of stimulation). These impressive results are achieved in only  $T = 0.4$  seconds of stimulation with using  $N_s = 3$  sub-bands. *The fact that we observe such impressive results with the same exact setting in both of these independent datasets (especially  $T = 0.4$ ,  $N_s = 3$  and the same DNN architecture as well as the same pre-processing parameter setting) is particularly important and thereby providing further reassurance about the robustness of our presented results.* In fact, across all stimulation durations  $T \in \{0.2, 0.3, \dots, 0.9, 1.0\}$

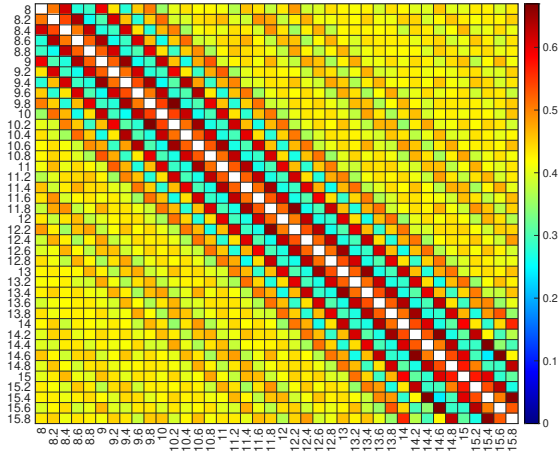


Fig. 8: The matrix  $M_D$  of the mean absolute distances for any pair of contrast modulating sinusoids with frequencies  $\{8, 8.2, \dots, 15.6, 15.8\}$  that are used for frequency tagging in the BCI SSVEP spellers of the both benchmark [16] and the BETA [17] datasets. Namely,  $M_D(i, j) = \frac{1}{T \times R} \sum_{k=0}^{T \times R - 1} |s(f_i, \theta_i, k) - s(f_j, \theta_j, k)|$ , where  $s(f, \theta, k) = \frac{1}{2}(1 + \sin 2\pi f(k/R) + \theta)$ ,  $R = 60$  Hz is the refresh rate of the monitor and  $T$  is the stimulation duration. The distance is the smallest when two frequencies are 0.6 or 0.8 Hz apart, and the largest when 0.2, 0.4 or 1 Hz apart. This pattern has an important effect on how the speller errors happen. Please see the text for details.

(not only at  $T = 0.4$  seconds), the proposed DNN uniformly and strongly outperforms all the other techniques in terms of both the accuracy and ITR, and this is true for both of the datasets. That the ITR is lower in the case of the BETA dataset is because of the low SNR of the BETA dataset since it was recorded outside of the laboratory environment.

**Remark:** Note that we compare against TSCORRCA, m-Extended-CCA, CORRCA and Standard-CCA with the benchmark dataset, whereas we compare against ms-eTRCA, eTRCA, m-Extended-CCA, Extended-CCA and ITTCA with the BETA dataset. The two sets of compared methods are not the same. This is because the results of a compared method (e.g. TSCORRCA) are available often for only one of the datasets (e.g. the benchmark for the TSCORRCA method). We opt to not test such a method with the dataset that the results are missing for, because it would be unfair if we tested as it might be necessary to optimize (for example, in terms of the pre-processing and parameter settings) and modify the methods for each different dataset. For this reason, in our comparisons, we only use the performance figures that are provided by the authors. Namely, we follow the same experimental procedure in their respective articles of these compared methods and therefore we repeat the same exact testing framework in [9] for Fig. 4 and the one in [17] for Fig. 6 for fairness (hence our two sets of compared methods here differ).

**Remark:** The eTRCA and the m-Extended-CCA methods are reported in [8] and in [12] to achieve 325.33 bits/min and 267 bits/min ITR performances, respectively. However, we point out that these performance figures are reported not with the datasets (the benchmark and BETA) that we here study with, but instead reported with their own datasets that are not publicly available. As Fig. 4 and Fig. 6 clearly show, the proposed DNN strongly outperforms these two

methods in our experiments on the publicly available large scale benchmark and BETA datasets.

As for the inter-class confusions presented in Fig. 5 and Fig. 7 for our best multi-class classification at  $T = 0.4$  seconds of stimulation and  $C = 64$  channels, we immediately observe two prominent error patterns.

The first pattern is that there exists a pronounced rate of error diagonally along the two lines  $f_{\text{true}} = f_{\text{predict}} \pm 0.6$  whereas this pattern completely disappears at even the adjacent closest neighbors of  $f_{\text{true}} = f_{\text{predict}} \pm 0.2$  or  $f_{\text{true}} = f_{\text{predict}} \pm 0.4$ . This is surprising at the first look as one would expect to confuse the target character with the character of the closest frequency. The reason that we discover for this finding is the following. The mean absolute distance between the samples (after sampling with the monitor refresh rate that is 60 Hz), which multiply the luminance of the character thumbnails as shown in Fig. 1, from two contrast modulating (i.e. frequency tagging) sinusoids with the frequencies  $f_1$  and  $f_2$  is the smallest when the frequencies are chosen as  $f_2 = f_1 \pm 0.6$  whereas it is the largest when chosen as  $f_2 = f_1 \pm 0.2$  or  $f_2 = f_1 \pm 0.4$ . This is clearly demonstrated in the matrix of distances in Fig. 8, and please see the strong correlation between the pattern in the distance matrix of Fig. 8 and the pattern in the confusion matrices of Fig. 5 and Fig. 7. Consequently, during stimulation, the luminance variations falling onto the retina and the corresponding early projections to the visual cortex are maximally similar when the frequencies are  $f_1$  and  $f_1 \pm 0.6$  and maximally dissimilar when the frequencies are  $f_1$  and  $f_1 \pm 0.2$  or  $f_1$  and  $f_1 \pm 0.4$ . This similarity in the luminance appears to (marginally though) reduce the discrimination power and hence negatively affect the recognition performance; but of course the dominating factor is still, thankfully, the stimulation frequency providing us at the end with an impressive rate of correct classification as shown right on the diagonal of the confusion matrices.

This first pattern is perhaps best understood with the vertical intermodulations (IM) resulting from the layout used in the character matrix, which emerges in our study as the second error pattern that is uniformly observed in the confusion matrix (Fig. 5) of the benchmark dataset. The source of confusion by this second error pattern is the well-known intermodulation phenomenon (cf. [49] and the references therein) which generates the IM components in the SSVEP spectrum at the integer multiples of the spatially nearby flickering frequencies that the subject is exposed to. If an IM is generated that is close to the frequency of a non-target character and also close to the one of the target character itself, then there seems to happen an error due to confusion. Since this is consistently and strongly observed in the confusion matrix (Fig. 5) of the benchmark dataset, we present as an important finding of our study that the vertical intermodulation, together with the first pattern of sinusoidal distances, has an important effect on how the errors happen in an emphasizing-the-first-pattern (if the IM exists) or suppressing-the-first-pattern (if the IM does not exist) manner. Namely, the relatively large rate of confusion in the first pattern between the frequencies  $f_1$  (predicted frequency) and  $f_2$  (true frequency) is persistent, A) only when the target character ( $f_2$  for  $f_2 = f_1 + 0.6$ ) is on the third, fourth and the fifth rows of the character matrix

	Benchmark [16]	BETA [17]
1 sub-band	77.89 ± 2.89	64.98 ± 2.25
2 sub-bands	78.80 ± 2.92	66.84 ± 2.17
3 sub-bands	79.89 ± 2.81	67.52 ± 2.17
4 sub-bands	79.86 ± 2.89	67.54 ± 2.12
5 sub-bands	79.96 ± 2.82	67.66 ± 2.17

TABLE 1: The mean classification accuracy (%), with the standard error, of our DNN is reported versus the varying number of sub-bands with 9 channels and 0.4 seconds of stimulation.

(Fig. 2) and also B) only when the target character ( $f_2$  for  $f_2 = f_1 - 0.6$ ) is on the first, second or the third rows of the character matrix (Fig. 2). We attribute this to the interference by the fifth degree vertical intermodulations generated in the both cases of A and B: In the case A, the confusing predicted frequency  $f_1$  can be obtained as the 5th IM  $f_1 = 3 \times f_2 - f_2^{u1} - f_2^{u2}$ , and in the case B,  $f_1$  can be obtained as the 5th IM  $f_1 = 3 \times f_2 - f_2^{l1} - f_2^{l2}$ . Here,  $u_k$  or  $l_k$  are the  $k$ th upper or lower adjacent neighbor frequency in the character matrix for  $k = 1$  or  $k = 2$ . Note that we do not observe a detrimental intermodulation when the target character (if it is on the first or second rows in the case A, and if it is on the fourth and fifth rows in the case B) does not have two vertical adjacent neighbors. Additionally, a detrimental intermodulation is not observed horizontally or also not observed at lower degrees (lower than 5) because of not that the horizontal and lower degree IMs are not generated (they are certainly generated) but that they are not any close to the frequency of the target character. Hence, an error does not happen in that specific way. We emphasize that the intermodulation effect is specific to the character matrix used in the stimulation. For this reason, we do not observe the same exact second pattern in the keyboard presentation of the BETA dataset (cf. Fig. 7) as the characters in that case are placed shuffled on the matrix. Hence, these two error patterns can provide key insights to the matrix and stimulation design in future studies.

In the rest of our performance evaluations, we fix the stimulation duration to  $T = 0.4$  seconds, i.e., signal length, as it yields the maximum ITR in both of the datasets. In addition, the ITR is an invertible function of the multi-class classification accuracy at a fixed stimulation duration; hence, to save space, we continue below with reporting only the accuracy since it is a direct performance measure with a more intuitive interpretation.

As reported in Table 1, for both of the datasets, using  $N_s = 3$  sub-bands with  $C = 9$  channels improves the accuracy by about 2 – 2.5% (which is significant when the standard error is inspected since  $N_s = 1$  and  $N_s = 3$  are separated by 1 unit of standard error, and also note that the chance level is  $1/M = 1/40 = 2.5\%$ ) compared to using  $N_s = 1$  sub-band only. Whereas using 2 more sub-bands with  $N_s = 5$  neither improves the accuracy nor does it degrade. This indicates that the first three harmonics should indeed be taken into account differently by an appropriate combination or normalization as we do in the first layer of the proposed DNN. In contrast, harmonics beyond the third degree can be grouped and processed together.

Therefore, we continue with using  $N_s = 3$  sub-bands in the following as it seems reasonable.

	Benchmark [16]	BETA [17]
3 channels	51.04 ± 4.09	42.73 ± 2.60
6 channels	74.55 ± 3.12	58.86 ± 2.49
9 channels	79.89 ± 2.81	67.52 ± 2.17
64 channels	84.54 ± 2.08	69.54 ± 2.07

TABLE 2: The mean classification accuracy (%), with the standard error, of our DNN is reported versus the varying number of channels with 3 sub-bands and 0.4 seconds of stimulation.

On the other hand, Table 2 reports the accuracy when using 3 (O1, Oz, O2), 6 (O1, Oz, O2, POz, PO3, PO4) and 9 (Pz, PO3, PO5, PO4, PO6, POz, O1, Oz, O2) channels as suggested by the study [36], as well as when using all 64 channels. We observe that using all 64 channels significantly improves the accuracy but that also reduces the practicality from the user’s point of view (since wearing all the electrodes might be inconvenient). Second, our DNN also works fairly well with 3 and 6 channels, which indicates that our algorithm can also be successfully used in the case of portable more practical systems where only a few channels can be used. Overall, using 9 channels is a reasonable choice in this trade-off between the accuracy and practicality.

Hence, we offer the proposed DNN with the default settings of  $T = 0.4$  seconds of stimulation,  $N_s = 3$  sub-bands and  $C = 9$  channels (Pz, PO3, PO5, PO4, PO6, POz, O1, Oz, O2).

Lastly, we study the importance of the electrodes (i.e. channels), in terms of their contribution to the target identification accuracy, by analyzing the channel combinations learned by the proposed DNN. For this purpose, in this part, we concentrate on 3 best combinations (since analyzing all 120 combinations given by the network would not be practical) such that for instance a large weight (in absolute value) in the combinations for a channel indicates a high importance. Note that in the current setting, our network learns 120 channel combinations in its second layer (in which the output is of size  $1 \times 50 \times 120$ , cf. Fig. 1) for the best achievable accuracy but does not rank them with respect to their importance to the accuracy. Hence, currently, it is not possible (without a post-component analysis of the 120 combinations which is not in the scope of the presented work) to immediately choose the most important 3 combinations out of those 120 ones. Nevertheless, in this part only, in order to have the network determine the best 3 combinations, we set the size of the second layer output as  $1 \times 50 \times 3$  instead of the original size  $1 \times 50 \times 120$  (cf. Fig. 1), and then train the network based on the entire set of available data (hence here we do not report accuracy since we do not use testing) when fed with all available 64 channels. Based on this approach, Fig. 9 presents the topographic maps of the best 3 channel combinations (without ranking them) that are learned by the proposed DNN in the case of the both datasets (the benchmark and BETA). In Fig. 9, each channel has a color closer to red (blue) if it has proportionally higher (lower) weight in the absolute value. We first observe that the channels that are recommended in the study [36] are also mostly covered by our network, which is an independent verification of a previous result. Therefore, this indicates that our network does not or limitedly overfit. However, unlike [36], we do not recommend the channel O1. Addi-



- interfaces," *IEEE Engineering in Medicine and Biology Magazine*, vol. 25, no. 5, pp. 32–38, 2006.
- [15] W. Wu, Z. Chen, X. Gao, Y. Li, E. N. Brown, and S. Gao, "Probabilistic common spatial patterns for multichannel eeg analysis," *IEEE Transactions on Pattern Analysis and Machine Intelligence*, vol. 37, no. 3, pp. 639–653, 2015.
- [16] Y. Wang, X. Chen, X. Gao, and S. Gao, "A benchmark dataset for ssvep-based brain-computer interfaces," *IEEE Transactions on Neural Systems and Rehabilitation Engineering*, vol. 25, no. 10, pp. 1746–1752, 2016.
- [17] B. Liu, X. Huang, Y. Wang, X. Chen, and X. Gao, "Beta: A large benchmark database toward ssvep-bci application," *Frontiers in Neuroscience*, vol. 14, p. 627, 2020.
- [18] Wang Yijun, Wang Ruiping, Gao Xiaorong, and Gao Shang kai, "Brain-computer interface based on the high-frequency steady-state visual evoked potential," *First International Conference on Neural Interface and Control*, pp. 37–39, 2005.
- [19] O. Friman, I. Volosyay, and A. Graser, "Multiple channel detection of steady-state visual evoked potentials for brain-computer interfaces," *IEEE Transactions on Biomedical Engineering*, vol. 54, no. 4, pp. 742–750, 2007.
- [20] Z. Lin, C. Zhang, W. Wu, and X. Gao, "Frequency recognition based on canonical correlation analysis for ssvep-based bcis," *IEEE Transactions on Biomedical Engineering*, vol. 53, no. 12, pp. 2610–2614, 2006.
- [21] W. Nan, C. M. Wong, B. Wang, F. Wan, P. U. Mak, P. I. Mak, and M. I. Vai, "A comparison of minimum energy combination and canonical correlation analysis for ssvep detection," *International IEEE/EMBS Conference on Neural Engineering*, pp. 469–472, 2011.
- [22] Y. Wang, M. Nakanishi, Y. Wang, and T. Jung, "Enhancing detection of steady-state visual evoked potentials using individual training data," *IEEE International Conference of Engineering in Medicine and Biology Society*, pp. 3037–3040, 2014.
- [23] Y. Zhang, G. Zhou, J. Jin, M. Wang, X. Wang, and A. Cichocki, "L1-regularized multiway canonical correlation analysis for ssvep-based bci," *IEEE Transactions on Neural Systems and Rehabilitation Engineering*, vol. 21, no. 6, pp. 887–896, 2013.
- [24] G. Bin, X. Gao, Y. Wang, Y. Li, B. Hong, and S. Gao, "A high-speed BCI based on code modulation VEP," *Journal of Neural Engineering*, vol. 8, no. 2, p. 025015, 2011.
- [25] Y. Zhang, G. Zhou, Q. Zhao, A. Onishi, J. Jin, X. Wang, and A. Cichocki, "Multiway canonical correlation analysis for frequency components recognition in ssvep-based bcis," *Neural Information Processing*, pp. 287–295, 2011.
- [26] Y. Zhang, G. Zhou, J. Jin, X. Wang, and A. Cichocki, "Frequency recognition in ssvep-based bci using multiset canonical correlation analysis," *International Journal of Neural Systems*, vol. 24, p. 1450013, 2014.
- [27] J. Pan, X. Gao, F. Duan, Z. Yan, and S. Gao, "Enhancing the classification accuracy of steady-state visual evoked potential-based brain-computer interfaces using phase constrained canonical correlation analysis," *Journal of Neural Engineering*, vol. 8, no. 3, p. 036027, 2011.
- [28] P. Poryzala and A. Materka, "Cluster analysis of cca coefficients for robust detection of the asynchronous ssveps in brain-computer interfaces," *Biomedical Signal Processing and Control*, vol. 10, pp. 201–208, 2014.
- [29] M. Nakanishi, Y. Wang, Y.-T. Wang, Y. Mitsukura, and T.-P. Jung, "A high-speed brain speller using steady-state visual evoked potentials," *International Journal of Neural Systems*, vol. 24, no. 06, p. 1450019, 2014.
- [30] M. Nakanishi, Y. Wang, Y.-T. Wang, and T.-P. Jung, "A comparison study of canonical correlation analysis based methods for detecting steady-state visual evoked potentials," *PLOS ONE*, vol. 10, no. 10, pp. 1–18, 2015.
- [31] X. Chen, Y. Wang, S. Gao, T.-P. Jung, and X. Gao, "Filter bank canonical correlation analysis for implementing a high-speed SSVEP-based brain-computer interface," *Journal of Neural Engineering*, vol. 12, no. 4, p. 046008, 2015.
- [32] F.-C. Lin, J. K. Zao, K.-C. Tu, Y. Wang, Y.-P. Huang, C.-W. Chuang, H.-Y. Kuo, Y.-Y. Chien, C.-C. Chou, and T.-P. Jung, "Snr analysis of high-frequency steady-state visual evoked potentials from the foveal and extrafoveal regions of human retina," *IEEE International Conference of Engineering in Medicine and Biology Society*, pp. 1810–1814, 2012.
- [33] C. M. Wong, F. Wan, B. Wang, Z. Wang, W. Nan, K. F. Lao, P. U. Mak, M. I. Vai, and A. Rosa, "Learning across multi-stimulus enhances target recognition methods in SSVEP-based BCIs," *Journal of Neural Engineering*, vol. 17, no. 1, p. 016026, 2020.
- [34] Y. Zhang, E. Yin, F. Li, Y. Zhang, D. Guo, D. Yao, and P. Xu, "Hierarchical feature fusion framework for frequency recognition in ssvep-based bcis," *Neural Networks*, vol. 119, pp. 1–9, 2019.
- [35] N.-S. Kwak, K.-R. Müller, and S.-W. Lee, "A convolutional neural network for steady state visual evoked potential classification under ambulatory environment," *PLOS ONE*, vol. 12, no. 2, pp. 1–20, 2017.
- [36] J. J. Podmore, T. P. Breckon, N. K. N. Aznan, and J. D. Connolly, "On the relative contribution of deep convolutional neural networks for ssvep-based bio-signal decoding in bci speller applications," *IEEE Transactions on Neural Systems and Rehabilitation Engineering*, vol. 27, no. 4, pp. 611–618, 2019.
- [37] N. Waytowich, V. J. Lawhern, J. O. Garcia, J. Cummings, J. Faller, P. Sajda, and J. M. Vettel, "Compact convolutional neural networks for classification of asynchronous steady-state visual evoked potentials," *Journal of Neural Engineering*, vol. 15, no. 6, p. 066031, 2018.
- [38] A. Ravi, N. H. Beni, J. Manuel, and N. Jiang, "Comparing user-dependent and user-independent training of CNN for SSVEP BCI," *Journal of Neural Engineering*, vol. 17, no. 2, p. 026028, 2020.
- [39] M. Attia, I. Hettiarachchi, M. Hossny, and S. Nahavandi, "A time domain classification of steady-state visual evoked potentials using deep recurrent-convolutional neural networks," *IEEE International Symposium on Biomedical Imaging*, pp. 766–769, 2018.
- [40] J. Thomas, T. Maszczyk, N. Sinha, T. Kluge, and J. Dauwels, "Deep learning-based classification for brain-computer interfaces," *IEEE International Conference on Systems, Man, and Cybernetics*, pp. 234–239, 2017.
- [41] K. He, X. Zhang, S. Ren, and J. Sun, "Deep residual learning for image recognition," *IEEE International Conference on Computer Vision and Pattern Recognition*, pp. 770–778, 2016.
- [42] T. Young, D. Hazarika, S. Poria, and E. Cambria, "Recent trends in deep learning based natural language processing," *IEEE Computational Intelligence Magazine*, vol. 13, no. 3, pp. 55–75, 2018.
- [43] R. Zerafa, T. Camilleri, O. Falzon, and K. P. Camilleri, "To train or not to train? a survey on training of feature extraction methods for SSVEP-based BCIs," *Journal of Neural Engineering*, vol. 15, no. 5, p. 051001, 2018.
- [44] M. Krauledat, M. Tangermann, B. Blankertz, and K.-R. Müller, "Towards zero training for brain-computer interfacing," *PLOS ONE*, vol. 3, no. 8, pp. 1–12, 2008.
- [45] F. A. B. Ramesh Srinivasan and P. L. Nunez, "Steady-state visual evoked potentials: Distributed local sources and wave-like dynamics are sensitive to flicker frequency," *Brain Topography*, vol. 18, no. 1, pp. 167–187, 2006.
- [46] J. R. Wolpaw, N. Birbaumer, D. J. McFarland, G. Pfurtscheller, and T. M. Vaughan, "Brain-computer interfaces for communication and control," *Clinical Neurophysiology*, vol. 113, no. 6, pp. 767–791, 2002.
- [47] N. Gordon, J. Hohwy, M. J. Davidson, J. J. van Boxtel, and N. Tsuchiya, "From intermodulation components to visual perception and cognition," *NeuroImage*, vol. 199, pp. 480–494, 2019.
- [48] D. P. Kingma and J. Ba, "Adam: A method for stochastic optimization," *arXiv*, 2014.
- [49] N. Alp, P. J. Kohler, N. Kogo, J. Wagemans, and A. M. Norcia, "Measuring integration processes in visual symmetry with frequency-tagged eeg," *Scientific Reports*, vol. 8, pp. 1–11, 2018.
- [50] A. Delorme and S. Makeig, "Eeglab: an open source toolbox for analysis of single-trial eeg dynamics including independent component analysis," *Journal of Neuroscience Methods*, vol. 134, no. 1, pp. 9–21, 2004.